J. Phys. B: At. Mol. Phys. **15** (1982) 119–142. Printed in Great Britain

Relativistic effects in electron scattering by atoms III. Elastic scattering by krypton, xenon and radon

L T Sin Fai Lam

Electron and Ion Diffusion Unit, Research School of Physical Sciences, Australian National University, Canberra, ACT 2600, Australia

Received 9 April 1981, in final form 29 June 1981

Abstract. The elastic scattering of electrons by krypton, xenon and radon atoms in the low-energy region up to 30 eV has been investigated. Direct and indirect relativistic effects are taken into account. The increase in the contribution of the direct effect with the nuclear charge of the target has been studied. Polarisation is included using a procedure based on the Pople–Schofield approximation. Partial-wave phaseshifts with $l = 0$–8 are presented. The calculation predicts results which are in quite good agreement with measurements on total, momentum-transfer and elastic differential cross sections for krypton and xenon. There is poor agreement between theory and experiment on spin polarisation for xenon at energies of 25 and 30 eV. The present work indicates that radon exhibits the Ramsauer–Townsend effect also.

1. Introduction

Studies of collisions of slow electrons with rare-gas atoms have been of great interest since the 1920's when early experiments (Townsend and Bailey 1922, Ramsauer 1923, Ramsauer and Kollath 1929) revealed pronounced minima in the total cross sections σ_T for electrons colliding with argon, krypton and xenon at energies in the vicinity of 0.5 eV. These structures in the cross sections are due to diffraction effects arising from the quantum-mechanical nature of matter and are now referred to as Ramsauer–Townsend effects or often simply as Ramsauer minima.

Rare-gas atoms are often used in experimental studies because they are inert and readily available. Extensive investigations have been made on σ_T using beam experiments (Wagenaar 1978, Dababneh *et al* 1980), on total momentum transfer cross sections σ_m using a swarm experiment (Frost and Phelps 1964) and on angular-scattering distributions (Mehr 1967, Heindorff *et al* 1976). Measurements of the absolute elastic differential cross sections have been made by Williams and Crowe (1975) and Srivastava *et al* (1981). There are also a few experiments on the spin polarisation of electrons scattered by inert gases (Mehr 1967, Klewer *et al* 1979). A survey of previous experimental and theoretical work on electron scattering by atoms at intermediate energies is given in a recent review paper by Bransden and McDowell (1978). An analysis and evaluation of cross sections for total scattering by noble gases over a large energy range starting from about 20 eV has been made by de Heer *et al* (1979).

Interest in studies in electron scattering from inert gases has been increased recently by the development of rare-gas halide high power lasers. Another important feature of

0022-3700/82/010119+24$02.00

electron scattering studies is the information it provides for correlation with similar investigations concerning positron collisions. It is well known that the calculated phaseshifts for positron–atom collisions are very sensitive to the polarisation used because of the partial cancellation between the repulsive static potential and the attractive polarisation potential on the projectile (Massey *et al* 1966). All measurements on positron scattering by atoms have been done, up to now, using inert gases. Theoretical studies on electron scattering can give considerable insight into the polarisation potential to be used in the corresponding positron problem (Sin Fai Lam 1982).

In this paper we use the semi-relativistic method developed in earlier papers (Sin Fai Lam 1980, Sin Fai Lam and Baylis 1981, to be referred to hereafter as I and II respectively) to investigate the elastic scattering of low-energy electrons by Kr, Xe and Rn. Dirac–Fock (relativistic Hartree–Fock) wavefunctions are used to describe the atoms (Desclaux 1975). Polarisation is included using a procedure based on the Pople–Schofield method (Sin Fai Lam 1981, Sinfailam and Thompson 1971). The polarisation potential is calculated using the valence electrons ns, np$_{3/2}$ and np$_{1/2}$ with $n = 4$, 5 and 6 for Kr, Xe and Rn, respectively. Moreover, for Kr and Xe the polarisation potential is then normalised to give the experimental value of the dipole polarisability in the limit of $r \to \infty$. The un-normalised polarisation potential is used for radon since the estimated error in the 'recommended' value of its dipole polarisability is 50% (Miller and Bederson 1977). Note that, although the Dirac equation would provide a more satisfactory treatment of electron scattering by a heavy atom such as radon, the present work based on the semi-relativistic method has been extended to study radon because no other investigation has been reported.

The rest of the paper is as follows. In § 2 we give an outline of the semi-relativistic method. We present in § 3 the results for the phaseshifts, the total elastic cross sections σ_T^{el}, the elastic momentum-transfer cross sections σ_m^{el}, the elastic differential cross sections $d\sigma^{el}/d\Omega$ and the spin polarisation†.

2. Theory

2.1. The scattering equation

We consider elastic scattering of an electron with a closed-shell atom and include the ground state of the target only in the model (I and II). The radial part of the continuum wavefunction satisfies the integrodifferential equation (I and II) (atomic units are used throughout, except where otherwise specified),

$$\left(\frac{d^2}{dr^2} - \frac{l(l+1)}{r^2} + k^2\right) f_\kappa(r) = 2(-V_S(r) + V_P(r) + V_R(r)) f_\kappa(r) + 2W(r) f_\kappa(r) \tag{1}$$

where k is the wavenumber of the incident electron, and κ defines both the total angular momentum j and the orbital angular momentum l according to

$$j = |\kappa| - \tfrac{1}{2} \tag{2a}$$

† In the notation adopted here σ_T is the total cross section (summed over all final states), σ_T^{el} the total elastic cross section and σ_T^{in} the total inelastic cross section, so that $\sigma_T = \sigma_T^{el} + \sigma_T^{in}$. Similarly, σ_m is the total momentum-transfer cross section, σ_m^{el} the elastic momentum-transfer cross section and σ_m^{in} the inelastic momentum-transfer cross section, so that $\sigma_m = \sigma_m^{el} + \sigma_m^{in}$.

$$l = \begin{cases} \kappa & \text{if } \kappa > 0 \\ -\kappa - 1 & \text{if } \kappa < 0. \end{cases} \tag{2b}$$

The static potential in equation (1) is written as

$$V_S(r) = \frac{Z}{r} - \sum_{\substack{n'j' = \text{closed} \\ \text{group}}} (2j'+1)\left(\frac{1}{r}\int_0^r (P^2_{n'j'}(s) + Q^2_{n'j'}(s))\,\mathrm{d}s + \int_r^\infty (P^2_{n'j'}(s) + Q^2_{n'j'}(s))s^{-1}\,\mathrm{d}s\right) \tag{3}$$

where Z is the nuclear charge, and $P_{n'j'}(r)/r$ and $Q_{n'j'}(r)/r$ are the large and small radial components of the one-electron atomic orbital (Desclaux 1975). The term V_P is the polarisation potential and is calculated using the Pople–Schofield method. The direct relativistic effect V_R in the scattering process is taken to be the second-order Dirac potential

$$V_R(r) = -\frac{\alpha^2}{2}\left[V_S^2 - \frac{\kappa}{r(\gamma + 1 + \alpha^2 V_S)}\left(\frac{\mathrm{d}V_S}{\mathrm{d}r}\right) + \frac{1}{2(\gamma+1+\alpha^2 V_S)}\left(\frac{\mathrm{d}^2 V_S}{\mathrm{d}r^2}\right) - \frac{3\alpha^2}{4(\gamma+1+\alpha^2 V_S)^2}\left(\frac{\mathrm{d}V_S}{\mathrm{d}r}\right)^2\right] \tag{4}$$

where α is the Sommerfeld fine-structure constant. Here $\gamma = (1 - v^2/c^2)^{-1/2}$ where v is the electron velocity and c the velocity of light; γ is approximately equal to 1 for low energies.

The kernel operator $W(r)$ defines the exchange between the scattered electron with quantum numbers (j, μ, a) and a group of bound electrons (n', j', μ', a')

$$W(r)f_\kappa(r) = -\sum_{\substack{n'j' = \text{closed} \\ \text{group}}} \sum_\lambda \frac{(2j'+1)}{(2j+1)} (C^j_{1/2\ \lambda\ 1/2})^2 Y_\lambda(P_{n'j'}, f_\kappa; r) P_{n'j'}(r) \tag{5}$$

where $C^j_{1/2\ \lambda\ 1/2}$ is a Clebsch–Gordan coefficient (Sin Fai Lam and Baylis 1981). The small radial component Q of the electron orbital has been neglected in equation (5). The error in the approximation used may be expected to be small, since the Q component of the bound orbital is appreciable only for the innermost electrons which provide a small contribution to exchange. The functions $Y_\lambda(P, f; r)$ satisfy the second-order differential equation

$$\frac{\mathrm{d}^2(rY_\lambda)}{\mathrm{d}r^2} = \frac{\lambda(\lambda+1)}{r^2}(rY_\lambda) - \frac{(2\lambda+1)}{r}P(r)f(r). \tag{6}$$

2.2. Cross section and spin polarisation

The collision of an electron with a heavy or moderately heavy atom is described by two scattering amplitudes

$$f(\theta) = \frac{1}{2\mathrm{i}k}\sum_{l=0}^\infty \{(l+1)[\exp(\mathrm{i}2\eta_l^+) - 1] + l[\exp(\mathrm{i}2\eta_l^-) - 1]\}P_l(\cos\theta) \tag{7a}$$

$$g(\theta) = \frac{1}{2\mathrm{i}k}\sum_{l=0}^\infty [\exp(\mathrm{i}2\eta_l^-) - \exp(\mathrm{i}2\eta_l^+)]P_l^1(\cos\theta) \tag{7b}$$

where $P_l(\cos\theta)$ and $P_l^1(\cos\theta)$ are the Legendre and associated Legendre polynomials (Mott 1929), and the plus and minus superscripts denote spin-up and spin-down cases, respectively (I and II). For an unpolarised incident beam, the elastic differential cross section is given by

$$\frac{d\sigma^{el}}{d\Omega} = |f|^2 + |g|^2 \tag{8}$$

and the spin polarisation is written as

$$P(\theta) = i(fg^* - f^*g)/(|f|^2 + |g|^2). \tag{9}$$

The total elastic and the elastic momentum-transfer cross sections are defined respectively, (Sin Fai Lam 1980), as

$$\sigma_T^{el} = \frac{4\pi}{k^2}\sum_l [(l+1)\sin^2\eta_l^+ + l\sin^2\eta_l^-] \tag{10a}$$

$$\sigma_m^{el} = \frac{4\pi}{k^2}\sum_l \left(\frac{(l+1)(l+2)}{2l+3}\sin^2(\eta_l^+ - \eta_{l+1}^+) + \frac{l(l+1)}{2l+1}\sin^2(\eta_l^- - \eta_{l+1}^-) + \frac{l+1}{(2l+1)(2l+3)}\sin^2(\eta_l^+ - \eta_{l+1}^-)\right). \tag{10b}$$

3. Results and discussion

3.1. Phaseshifts

The results for s-wave scattering of slow electrons by Kr, Xe and Rn are shown in figure 1. Exchange plays an important role, and all orbitals have been used to calculate the contribution to exchange. We have calculated three sets of results: exchange only (curve A); exchange and polarisation (curve B); and exchange, polarisation and the direct relativistic effect (curve C). Comparison between curves B and C shows that the contribution from the direct relativistic effect is small for Kr, appreciable for Xe and very large for Rn. The increase in the importance of the direct effect with nuclear charge is to be expected. For s-wave scattering the direct relativistic effect is due mainly to the 'Darwin' and the relativistic mass corrections (I and II). We have also shown in figures 1(*a*) and 1(*b*) the recent calculations of Yau *et al* (1980) on Kr and Xe. Yau *et al* have used a polarised-orbital approximation calculated in a coupled Hartree–Fock scheme. In these calculations the target is described by a non-relativistic wavefunction, exchange is approximated by an equivalent local potential, and the polarisation potential is calculated using the valence electrons. Direct and indirect relativistic effects are not taken into account in their work. There is agreement between the present work (curve C) and the results of Yau *et al*. The present semi-relativistic calculation is also in good agreement with the full relativistic treatment of Walker (1981) for Kr and Xe. In the work of Walker the dipole polarisation of the valence electrons is calculated using the polarised-orbital method and the polarisation potential is then normalised to give the experimental value of the dipole polarisability.

We show in figure 2 our calculations on the p-wave scattering along with the results of Yau *et al* (1980) and Walker (1981) for Kr and Xe. In the present work we have used

in calculating exchange all orbitals for Kr and Xe, and orbitals with $n \geqslant 2$ for Rn. Again comparison between curve C (exchange and polarisation) and curves D and E (exchange, polarisation and direct relativistic effect for spin-up and spin-down cases respectively) shows that the contribution from the direct relativistic effect is small for

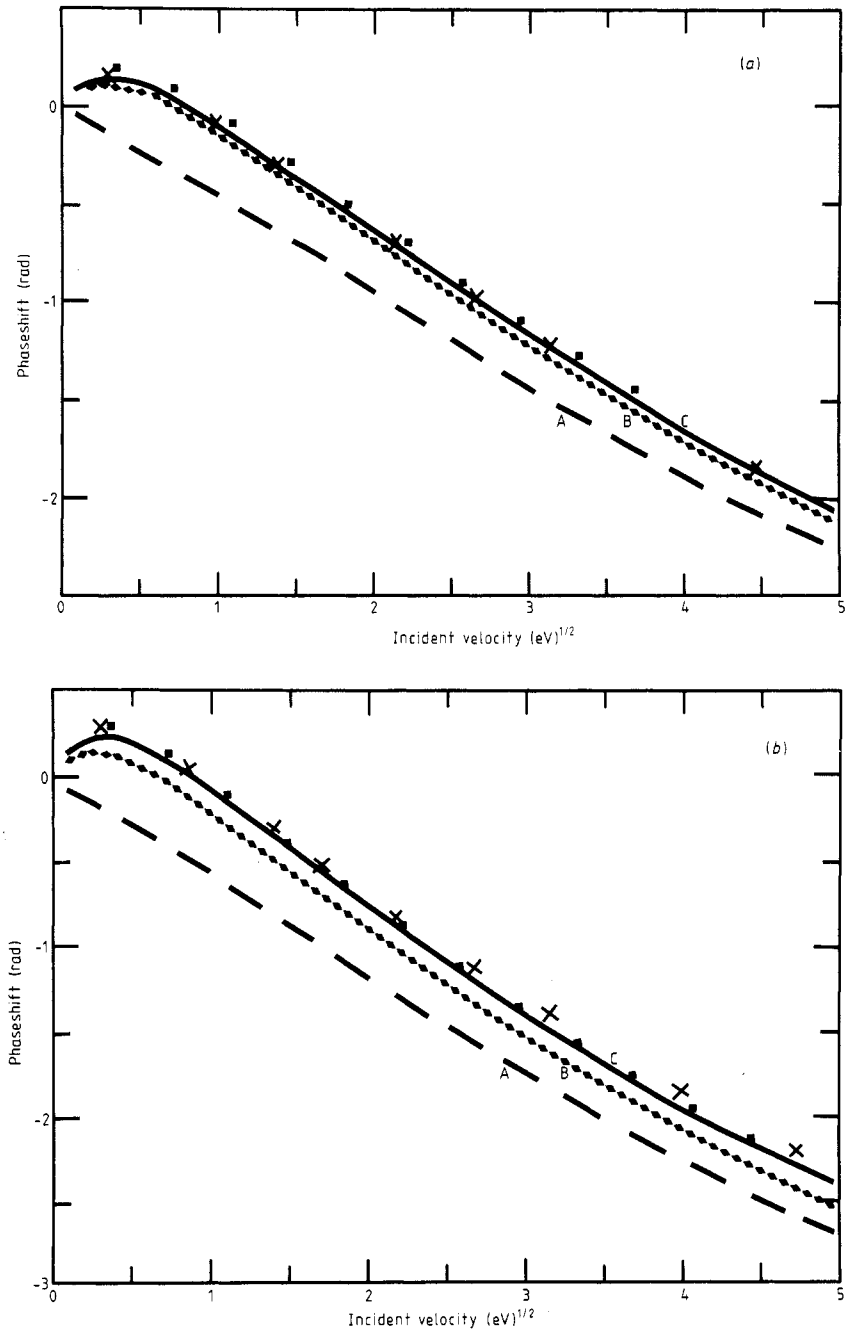

Figure 1.

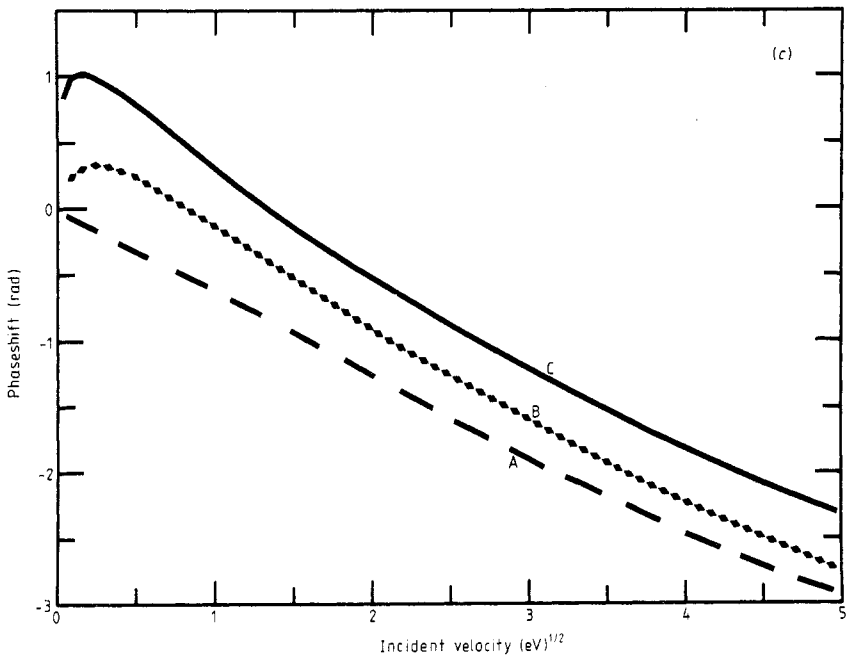

Figure 1. S-wave phaseshifts, (*a*) Kr, (*b*) Xe, (*c*) Rn. Present work: A, exchange; B, exchange and polarisation; C, exchange, polarisation and direct relativistic effect. ×, Walker (1981); ■, Yau *et al* (1980).

Kr, appreciable for Xe and very large for Rn†. The increase in importance of this effect with nuclear charge is seen again in the increase in the spin–orbit splitting of the phaseshift (curves D and E). Note that for $l > 0$ the direct relativistic effect is due mainly to the relativistic mass correction and the spin–orbit coupling terms. There is generally good agreement between the present work (curves D and E) and the non-relativistic calculations of Yau *et al.* There is excellent agreement between the present work (curve E) and the full relativistic calculation of Walker (1981) for Kr. The results of Walker for Xe are slighly larger than the present calculations, probably due to the somewhat more attractive polarisation potential used in his work. It will be shown later that this will have a very marked effect on the calculated f-wave phaseshift and will result in an 'artifact' in the predicted total elastic cross section σ_T^{el} at energies above 15 eV. However, the magnitude of the splitting of the p-wave phaseshifts for spin up and spin down is the same in both the present and in Walker's calculations for Kr and Xe. This indicates that the second-order Dirac potential is a good approximation to allow for the direct relativistic effect in the present work. The results for Rn (figure 2(*c*)) show that there is a substantial difference between the phaseshifts for the spin-up and spin-down cases calculated with exchange only (curves A and B) indicating that the indirect relativistic effect induces an appreciable spin polarisation (II). Note that for Kr and Xe the spin–orbit splitting of the phaseshift due to the indirect effect is negligible, and only the results for exchange for spin up are shown in figures 2(*a*) and 2(*b*).

† Note that, when only spin-up (or spin-down) phases are shown in figures 2–4, this means that the spin-up and spin-down phases are too close together to be plotted separately. However, for radon the results for exchange and polarisation for spin down (with $l > 0$) are not shown for reasons of clarity.

Figure 3 shows the calculations for the d-wave scattering. All orbitals have been used in calculating exchange for Kr and Xe, and orbitals with $n \geqslant 2$ for Rn. The direct relativistic effect is small, and consequently the spin–orbit splitting of the phaseshift is small. This is due to the fact that, although the magnitude of the second-order Dirac

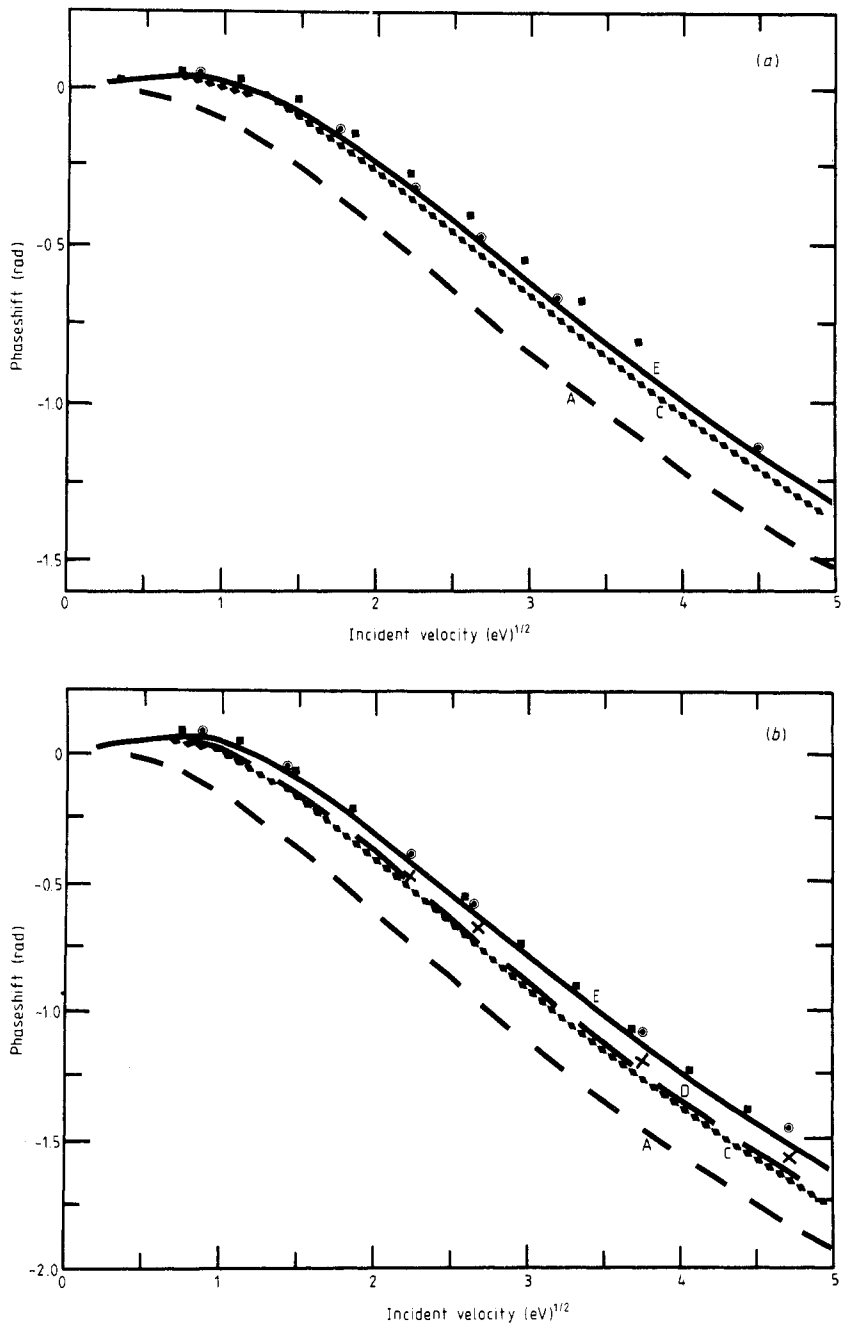

Figure 2.

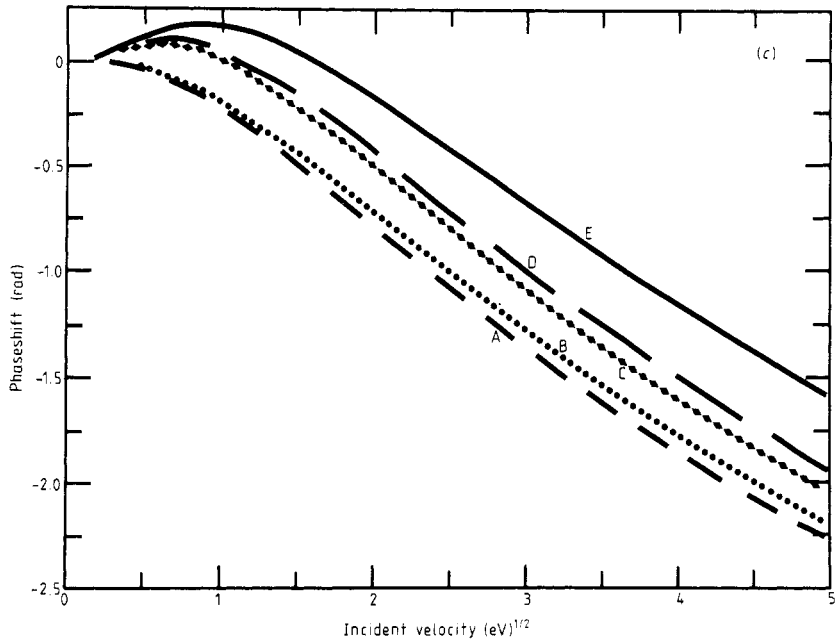

Figure 2. P-wave phaseshifts, (*a*) Kr, (*b*) Xe, (*c*) Rn. Present work: A, exchange (spin up); B, exchange (spin down); C, exchange and polarisation (spin up); D, exchange, polarisation and direct relativistic effect (spin up); E, exchange, polarisation and direct relativistic effect (spin down). ×, ⊙, spin-up and spin-down results of Walker (1981); ■, Yau *et al* (1980).

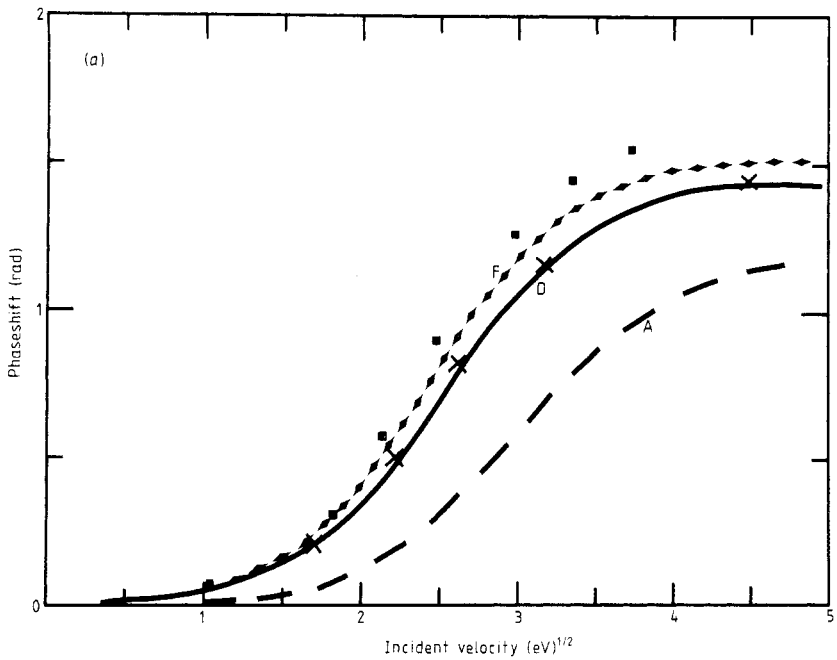

Figure 3.

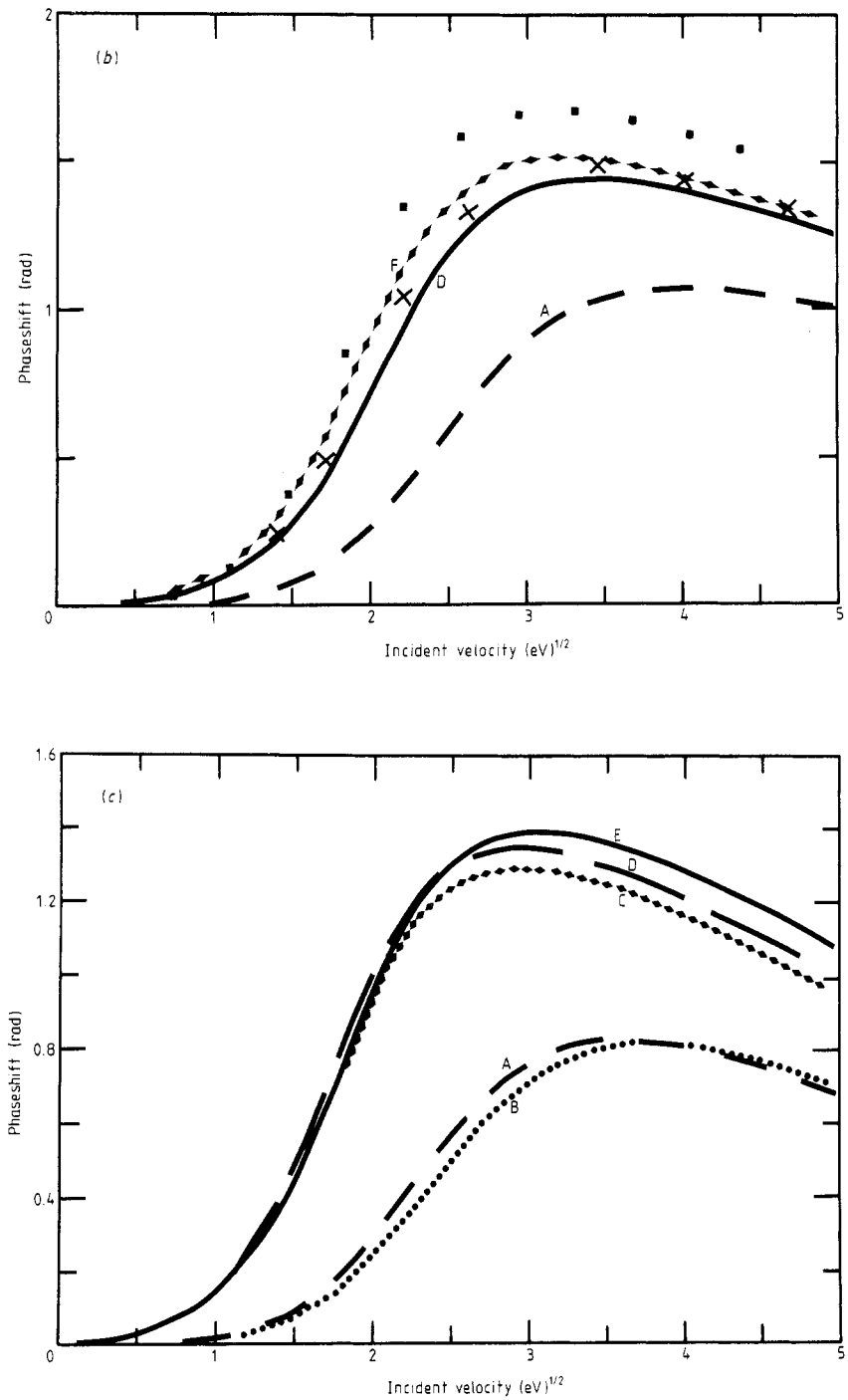

Figure 3. D-wave phaseshifts, (*a*) Kr, (*b*) Xe, (*c*) Rn. Present work: A, exchange (spin up); B, exchange (spin down); C, exchange and polarisation (spin up); D, exchange, polarisation and direct relativistic effect (spin up); E, exchange, polarisation and direct relativistic effect (spin down); F, exchange, *un-normalised* polarisation and direct relativistic effect (spin up). ×, spin-up results of Walker (1981); ■, Yau *et al* (1980).

potential increases with the orbital angular momentum l, its contribution to the scattering process decreases as the magnitude of the centrifugal barrier increases. It is again seen that the indirect effect causes a small spin–orbit splitting of the phaseshift for Rn (figure 3(c) curves A and B). There is again excellent agreement between the present work and the full relativistic treatment of Walker (1981) for Kr. The results of Walker for Xe are again somewhat larger than ours. We have shown also in figures 3(a) and (b) the calculations of Yau *et al* (1980) for Kr and Xe. The results of Yau *et al* are much higher than those of the present calculations (curve D) at energies above 4 eV. If direct and indirect relativistic effects were not included, the method used in the present work would be similar to the treatment used by Thompson (1971). For the electron–argon system comparison shows that the d- and f-wave phaseshifts of Yau *et al* are larger than those of Thompson.

We have also performed some calculations *without* normalising the polarisation potential in order to investigate further the discrepancy between the present work and the calculation of Yau *et al.* The effective potential is then more attractive and the predicted phaseshifts become larger (figures 3(a) and (b), curve F)†, but these results are still substantially smaller than the values of Yau *et al.* However, the use of the *un-normalised* polarisation potential (which gives a dipole polarisability larger than experimental value) is difficult to justify on physical grounds. For low-energy positron scattering from atoms, calculations using normalised and un-normalised polarisation potentials can give total elastic cross sections with different features. In the following paper (Sin Fai Lam 1982) we shall present results on positron–krypton systems which indicate a Ramsauer minimum using normalised polarisation and no evidence of such structure using *un-normalised* polarisation. The predicted phaseshifts are very sensitive to the polarisation used because of the partial cancellation between the repulsive static and the attractive polarisation potentials on the scattered particle (Massey *et al* 1966).

The differences between the present results and those of Yau *et al* may be due to several sources. In the work of Yau *et al* the static exchange kernels are approximated by an equivalent local exchange potential (Furness and McCarthy 1973). McCarthy *et al* (1977) have used a modified form of this method, and have calculated elastic differential cross sections for krypton and xenon at 20 and 30 eV which are in quite good agreement with the present work and with experiment (see § 3.3). As indicated previously, relativistic effects are not taken into account in the work of Yau *et al.* Another possible source of discrepancy is the polarisation potential. The polarisation potential calculated by Yau *et al* yields a dipole polarisability which is in good agreement with experiment (McEachran *et al* 1979). Contributions from higher multipole polarisabilities are included in their work. In the present work we have used only the dipole term which is then normalised to give the experimental value of the dipole polarisability. Thus the asymptotic forms of the polarisation potential used in the present calculation and of the corresponding dipole term used in the work of Yau *et al* are similar. However, their functional forms may be different and their contribution to collision processes may not be the same. We note also that it is difficult to assess the relative contribution to scattering due to the higher multipole terms used in the calculation of Yau *et al.* It seems that the *effective* potential (static, exchange and polarisation) is stronger in their calculation than in the present work. It will be shown that this will have a large effect on the predicted value of σ_T^{el}.

† Polarisation in our results for Kr and Xe implies that the polarisation potential has been *normalised*, unless otherwise specified.

We present in figure 4 the results for f-wave scattering. Exchange is calculated using orbitals with $n \geqslant 3$ for Kr and Xe, and $n \geqslant 4$ for Rn. The direct relativistic effect is negligible for all three atoms. The results of the calculations of Yau *et al* (1980) are again larger than our results for Kr and are much larger for Xe at energies above 4 eV. There is good agreement between the present work and the calculation of Walker

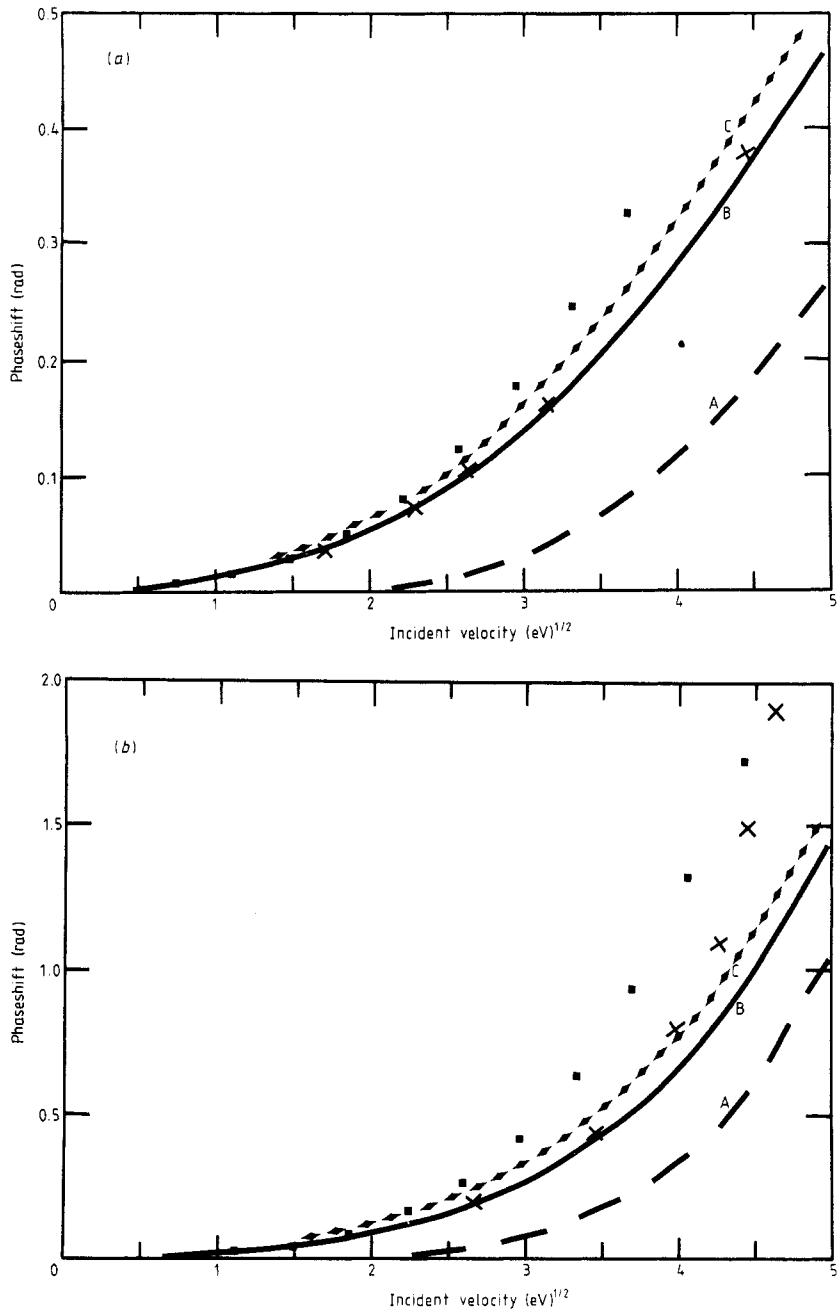

Figure 4.

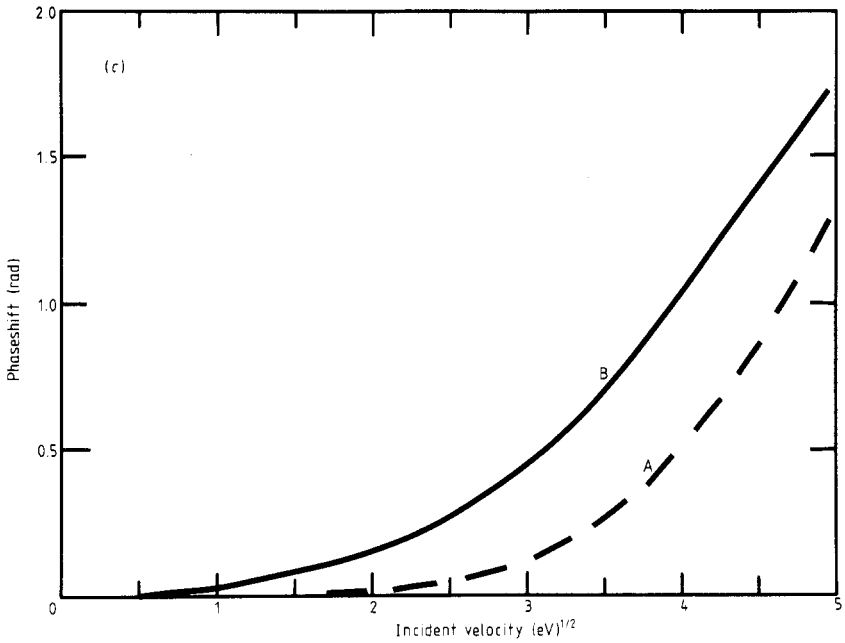

Figure 4. F-wave phaseshifts, (*a*) Kr, (*b*) Xe, (*c*) Rn. Present work: A, exchange (spin up); B, exchange and polarisation (spin up); C, exchange and *un-normalised* polarisation (spin up). ×, spin-up results of Walker (1981); ■ Yau *et al* (1980).

(1981) for Kr. For Xe the somewhat stronger polarisation potential used by Walker has a very marked effect on the f-wave scattering at energies above 15 eV where there is a broad shape resonance and the predicted phaseshift is much larger than ours. When the polarisation potential is not normalised in our calculation, the predicted phaseshifts are larger again (figures 4(*a*) and (*b*), curve C).

We list in tables 1–3 our calculated phaseshifts for partial-wave scattering with $l = 0$–8. The results have been obtained with exchange and polarisation, and for $l = 0$ to 2 with the direct relativistic effect included. For the partial waves $l = 4$–8, exchange has been calculated using orbitals $n = 4$, 5 and 6 for Kr, Xe and Rn respectively.

3.2. Total and momentum-transfer cross sections for elastic scattering

Figure 5 compares calculations on σ_T^{el} and experimental results (mostly for σ_T) for electron collisions with Kr. (All partial-wave phaseshifts with $l = 0$–8 have been used in the present work to calculate the total, momentum-transfer cross sections, and differential cross sections and spin polarisation for elastic scattering.) There is agreement between the present work and the results of Yau *et al* (1980) (calculated using partial waves $l = 0$ to 3) in the lower energy region. Both calculations reproduce the Ramsauer minimum in the vicinity of 0.7 eV (Ramsauer and Kollath 1929). However, the calculation of Yau *et al* is larger than the present work at energies above 4 eV. This discrepancy is due to the fact that their d- and f-wave phaseshifts are larger (figures 3(*a*) and 4(*a*)). In the higher energy region the dominant contribution to the cross section comes from these two partial-wave phaseshifts, and any overestimate in the calculated values is likely to have a large effect on the predicted cross section. There

Table 1. Phaseshifts for elastic scattering of electrons by krypton.

E(eV)	η_0(rad)	η_1^+	η_1^-	η_2^+	η_2^-	η_3	η_4	η_5	η_6	η_7	η_8
0.01	0.075 16	0.001 90	0.001 92	0.000 22	0.000 22	0.000 10					
0.05	0.119 78	0.010 48	0.010 66	0.001 86	0.001 86	0.000 64					
0.1	0.129 24	0.018 44	0.018 94	0.003 91	0.003 91	0.001 32	0.000 60	0.000 30	0.000 18	0.000 11	
0.2	0.115 49	0.025 51	0.026 85	0.008 06	0.008 06	0.002 65	0.001 21	0.000 60	0.000 36	0.000 23	
0.5	0.036 97	0.033 23	0.037 70	0.021 28	0.021 23	0.006 64	0.003 00	0.001 49	0.000 90	0.000 58	0.000 40
1	−0.095 55	0.012 03	0.021 77	0.046 25	0.045 97	0.012 91	0.005 85	0.003 00	0.001 80	0.001 17	0.000 80
2	−0.313 99	−0.071 41	−0.053 45	0.114 68	0.113 35	0.025 53	0.011 31	0.006 01	0.003 61	0.002 34	0.001 60
5	−0.769 51	−0.358 84	−0.327 80	0.493 84	0.487 05	0.069 20	0.028 52	0.015 10	0.009 00	0.005 82	0.003 96
10	−1.254 06	−0.727 85	−0.688 42	1.147 18	1.148 86	0.159 42	0.059 18	0.030 55	0.018 10	0.011 66	0.007 82
14	−1.530 98	−0.948 31	−0.905 96	1.342 66	1.350 73	0.241 92	0.085 15	0.043 13	0.025 38	0.016 19	0.010 84
20	−1.850 38	−1.205 28	−1.160 60	1.417 11	1.428 43	0.371 75	0.125 54	0.062 21	0.036 42	0.023 02	0.015 25
25	−2.062 00	−1.375 91	−1.330 17	1.415 76	1.427 87	0.478 28	0.159 76	0.078 20	0.045 35	0.028 64	0.018 82
30	−2.240 95	−1.520 06	−1.473 63	1.395 65	1.408 04	0.578 86	0.193 95	0.094 17	0.054 13	0.034 17	0.022 30

Table 2. Phaseshifts for elastic scattering of electrons by xenon.

E(eV)	η_0(rad)	η_1^+	η_1^-	η_2^+	η_2^-	η_3	η_4	η_5	η_6	η_7	η_8
0.01	0.135 12	0.003 55	0.003 61	0.000 48	0.000 48	0.000 19					
0.05	0.216 11	0.016 83	0.017 50	0.003 16	0.003 15	0.001 07					
0.1	0.229 22	0.025 34	0.027 16	0.006 51	0.006 51	0.002 16	0.000 98	0.000 49	0.000 30		
0.2	0.207 32	0.040 72	0.045 55	0.013 39	0.013 36	0.004 32	0.001 96	0.000 97	0.000 60		
0.5	0.091 81	0.046 60	0.061 86	0.036 34	0.036 06	0.010 81	0.004 88	0.002 44	0.001 48	0.000 97	0.000 65
1	−0.087 10	0.009 56	0.040 32	0.084 19	0.082 74	0.020 90	0.009 37	0.004 90	0.002 92	0.001 91	0.001 28
2	−0.365 72	−0.125 40	−0.073 26	0.237 59	0.230 50	0.042 50	0.018 41	0.009 83	0.005 80	0.003 81	0.002 56
5	−0.917 56	−0.512 82	−0.431 47	0.990 75	0.981 69	0.123 62	0.047 30	0.024 76	0.014 75	0.009 51	0.006 44
10	−1.483 80	−0.972 19	−0.873 89	1.398 45	1.420 50	0.319 88	0.100 05	0.050 38	0.029 59	0.019 04	0.012 90
14	−1.801 97	−1.238 73	−1.134 71	1.392 63	1.420 68	0.537 58	0.145 62	0.071 37	0.041 55	0.026 69	0.018 05
20	−2.166 11	−1.546 17	−1.437 74	1.304 41	1.335 13	0.998 59	0.216 98	0.103 37	0.059 48	0.038 13	0.025 75
25	−2.406 33	−1.749 64	−1.639 16	1.219 61	1.250 98	1.471 65	0.277 27	0.130 23	0.074 28	0.047 57	0.032 13
30	−2.608 94	−1.921 60	−1.809 76	1.137 11	1.168 74	1.195 19	0.336 88	0.157 07	0.088 94	0.056 93	0.038 38

Table 3. Phaseshifts for elastic scattering of electrons by radon.

E(eV)	η_0(rad)	η_1^+	η_1^-	η_2^+	η_2^-	η_3	η_4	η_5	η_6	η_7	η_8
0.01	0.972 26	0.006 35	0.006 61	0.000 91	0.000 91	0.000 33					
0.05	1.013 98	0.024 92	0.027 84	0.005 26	0.005 26	0.001 75					
0.1	0.945 50	0.045 89	0.053 95	0.010 75	0.010 70	0.003 58	0.001 60	0.000 79	0.000 49		
0.2	0.825 78	0.072 36	0.093 55	0.022 06	0.021 96	0.007 13	0.003 19	0.001 59	0.000 97		
0.5	0.573 50	0.099 98	0.164 10	0.060 17	0.058 98	0.017 55	0.007 86	0.004 00	0.002 41	0.001 63	0.001 20
1	0.299 35	0.054 42	0.175 25	0.143 01	0.136 27	0.034 36	0.015 12	0.008 02	0.004 82	0.003 17	0.002 24
2	−0.065 90	−0.105 87	0.080 85	0.404 10	0.371 81	0.070 70	0.030 24	0.016 10	0.009 64	0.006 25	0.004 33
5	−0.713 67	−0.554 08	−0.290 12	1.185 62	1.171 51	0.213 25	0.078 13	0.040 73	0.024 16	0.015 49	0.010 15
10	−1.340 86	−1.067 62	−0.763 47	1.330 46	1.388 57	0.530 67	0.162 24	0.082 45	0.048 49	0.030 86	0.020 51
14	−1.686 07	−1.361 78	−1.044 78	1.250 99	1.325 39	0.870 90	0.229 91	0.115 41	0.067 77	0.043 08	0.028 43
20	−2.078 24	−1.699 91	−1.373 33	1.103 21	1.187 77	1.396 69	0.327 91	0.162 85	0.095 66	0.060 80	0.039 95
25	−2.336 22	−1.923 67	−1.592 79	0.984 68	1.072 36	1.768 62	0.405 12	0.200 18	0.117 70	0.074 79	0.048 96
30	−2.553 84	−2.113 08	−1.779 38	0.874 91	0.964 26	2.006 28	0.478 06	0.235 58	0.138 53	0.088 02	0.057 36

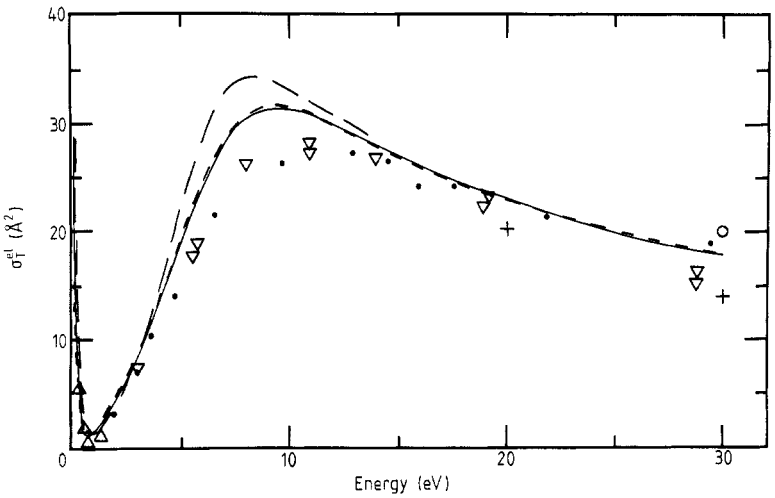

Figure 5. Total elastic cross sections for krypton. Theory: ——, present work; – –, Walker (1981); — —, Yau *et al* (1980), Experiment: △, Ramsauer and Kollath (1929); ▽, Ramsauer (1923); +, Williams and Crowe (1975); ○, Wagenaar (1978); ● Dababneh *et al* (1980).

is qualitative agreement between our calculated σ_T^{el} and the experimental data on σ_T (Ramsauer 1923, Wagenaar 1978, Dababneh *et al* 1980) in the higher energy region. The present cross section is larger than experiment by up to 15%, whereas the cross section of Yau *et al* is larger by up to 30%. The data of Williams and Crowe (1975) on σ_T^{el} at 20 and 30 eV (calculated from their measurements of elastic differential cross sections between 20 and 150°, see de Heer *et al* (1979)) are lower than the measurements of σ_T by Wagenaar (1978) and Dababneh *et al* (1980). The errors in the measurements of Wagenaar, Dababneh *et al*, and Williams and Crowe are ±4, ±11 and ±12% respectively. We have also shown in figure 5 the full relativistic calculations of Walker (1981), who has included exchange and polarisation. There is excellent agreement between the present semi-relativistic calculation and the full relativistic work of Walker throughout the whole energy range.

We present in figure 6 our calculations of the elastic momentum-transfer cross section σ_m^{el} for Kr along with the calculation of Yau *et al* (1980) and the measurements of σ_m by Frost and Phelps (1964). There is qualitative agreement between theory and experiment.

We compare in figure 7 our calculations of σ_T^{el} for Xe with those of Yau *et al* (1980), who have used partial waves with $l = 0$–3. There is again good agreement between these calculations in the lower energy region, and both reproduce the Ramsauer minimum in the vicinity of 0.7 eV (Ramsauer and Kollath 1929). However, at energies above 4 eV the cross section of Yau *et al* is larger than the present cross section. This discrepancy is again due to the dominant contributions from the d and f partial-wave phaseshifts which are larger in the calculations of Yau *et al* (figures 3(*b*) and 4(*b*)). We have also shown in figure 7 the measurements of σ_T by Ramsauer (1923), Wagenaar (1978), and Dababneh *et al* (1980), and of σ_T^{el} by Williams and Crowe (1975) (see de Heer *et al* 1979). Experiment is in better agreement with the present work than with the results of Yau *et al*, which can be larger than the measurements by up to 50%. There is good agreement between the present semi-relativistic calculation and the full

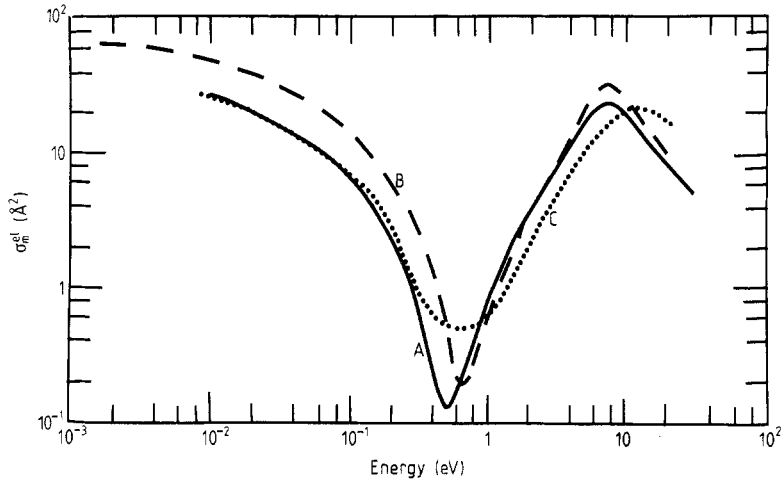

Figure 6. Elastic momentum-transfer cross sections for krypton. Theory: A, present work; B, Yau *et al* (1980). Experiment: C, Frost and Phelps (1964).

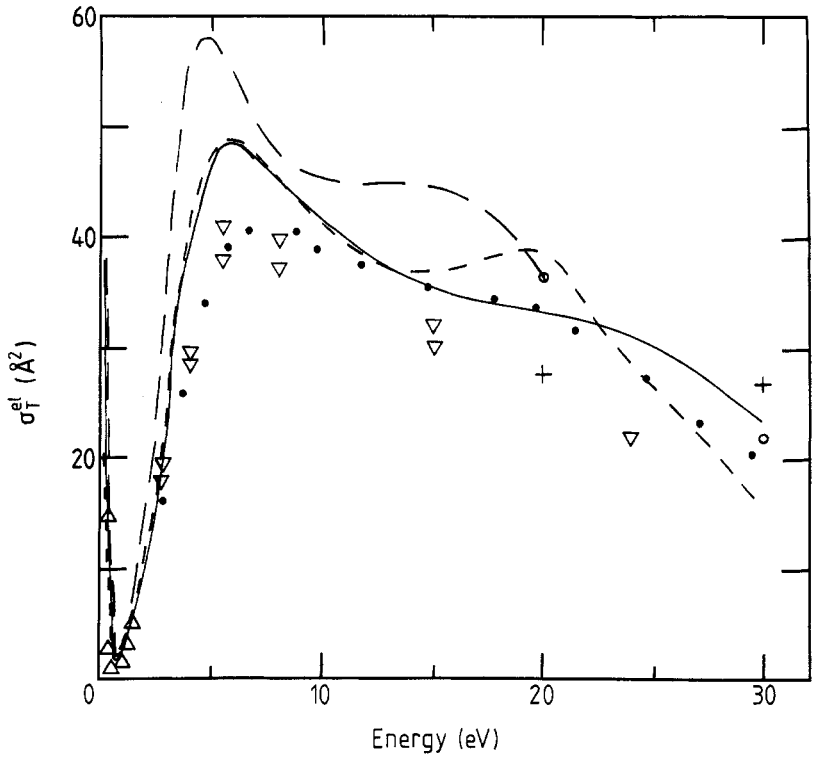

Figure 7. Total elastic cross sections for xenon. Theory: ——, present work; – –, Walker (1981); — —, Yau *et al* (1980). Experiment: △, Ramsauer and Kollath (1929); ▽, Ramsauer (1923); +, Williams and Crowe (1975); ○, Waganaar (1979); ● Dababneh *et al* (1980).

relativistic treatment of Walker (1981) for energies up to 15 eV. At higher energies his calculated cross section is larger than ours and exhibits a broad 'hump' before becoming smaller than our results at energies above 22 eV. This is due to the somewhat stronger polarisation potential in Walker's calculation which has a marked effect on the f-wave scattering.

Figure 8 compares the present results of σ_m^{el} for Xe with the calculation of Yau *et al* (1980) and the measurements of σ_m by Frost and Phelps (1964). We have listed in table 4 our calculated total and momentum-transfer cross sections for elastic scattering by Kr, Xe and Rn. It is seen from table 4 that there is a Ramsauer–Townsend effect for Rn in the vicinity of 1 eV. Note that the polarisation potential used for Rn may be over

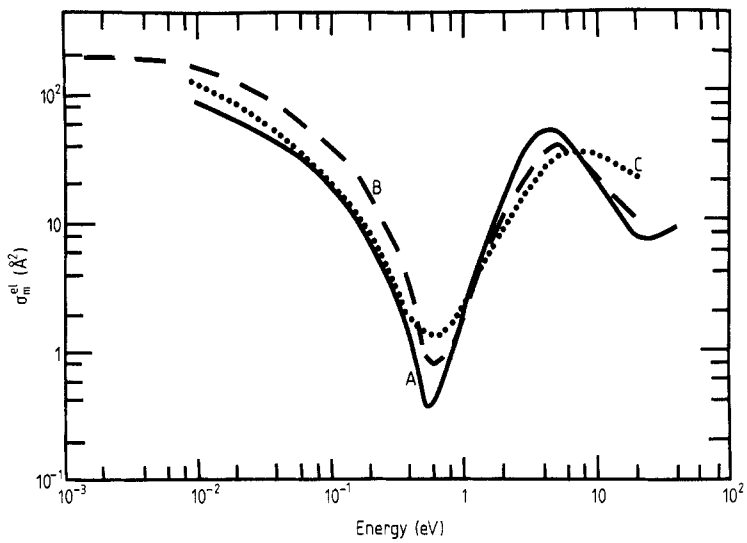

Figure 8. Elastic momentum-transfer cross sections for xenon. Theory: A, present work; B, Yau *et al* (1980). Experiment: C, Frost and Phelps (1964).

Table 4. Total and momentum-transfer cross sections for elastic scattering (Å^2).

	Kr		Xe		Rn	
E(eV)	σ_T^{el}	σ_m^{el}	σ_T^{el}	σ_m^{el}	σ_T^{el}	σ_m^{el}
0.01	27.05	25.67	87.07	82.47	3268.33	3239.26
0.05	14.01	11.53	44.92	37.83	692.16	668.42
0.1	8.49	6.05	25.81	19.91	318.47	293.79
0.2	3.76	2.09	11.69	6.93	134.63	112.16
0.5	0.74	0.10	2.32	0.42	34.64	19.79
1	1.06	0.85	2.33	1.56	11.14	4.36
2	4.30	3.57	10.83	9.70	19.37	16.36
5	19.07	17.11	46.98	37.48	54.94	39.67
10	31.48	20.28	41.37	18.42	47.30	16.25
14	28.01	13.58	36.03	10.94	44.61	9.73
20	22.83	8.16	33.15	6.97	38.36	9.66
25	19.83	5.87	30.15	8.16	30.23	11.45
30	17.63	4.47	23.33	9.90	23.21	11.45

estimated and consequently the position of the Ramsauer–Townsend effect predicted in the present work is likely to be higher than the actual value.

3.3 Elastic differential cross section and spin polarisation

There have been several measurements of angular distributions of electron scattering from rare-gas atoms, and the early data have been compiled by Kieffer (1971). However, the experimental results are relative and this disadvantage limits their value as a means of testing various theoretical models. Recently, absolute differential cross sections for elastic scattering have become available (Williams and Crowe 1975), and the data can be used for a sensitive comparison between theory and experiment.

We compare in figure 9 our calculated differential cross sections $d\sigma^{el}/d\Omega$ for elastic scattering of electrons from Kr at 20 and 30 eV with the experiment of Williams and Crowe (1975), and the theoretical results of McCarthy *et al* (1977) and Walker (1981). In the optical model calculation of McCarthy *et al* Hartree–Fock orbitals are used, exchange is treated by an equivalent local approximation, polarisation by a complex potential to allow for virtual excitation of inelastic channels, and the direct relativistic effect by the second-order Dirac potential. There is good agreement between the calculations and experiment. The full relativistic work of Walker (1981) is in excellent agreement with the present semi-relativistic calculation throughout the whole range of scattering angles.

Figure 10 compares our predicted differential cross sections for elastic scattering of electrons by Xe at 20 and 30 eV with the optical model calculation of McCarthy *et al* (1977), the full relativistic work of Walker (1981) and the absolute measurements of Williams and Crowe (1975). The experimental data provide a very sensitive test for comparing theoretical models, especially in the energy range 20–30 eV where there is a large contribution from both d and f partial-wave scattering. It is seen that there is very good agreement between experiment and the present work. Agreement with the full relativistic calculation of Walker is not satisfactory because of his larger f-wave phaseshift (see § 3.1). Our results for Rn at 20 and 30 eV are shown in figure 11.

Comparison of the results presented in figures 9–11 shows some interesting features. For Kr at 20 eV the elastic differential cross section exhibits minima near 70 and 130°, and a maximum near 100°. The d-wave phaseshift is large, so that the distribution is dominated by the harmonic $P_2(\cos\theta)$ with an appreciable contribution from $P_3(\cos\theta)$ due to the f-wave phaseshift. Both d- and f-wave phaseshifts are large for Xe at 20 eV, and the interference between these two contributions (and also with contributions from other partial waves) gives, in the differential cross section, three minima near 60, 100 and 150°. The f-wave phaseshift is even larger for Rn, and the three minima in the differential cross sections are deeper. The contribution from the f-wave phaseshift increases rapidly with energy, so that the minima in the differential cross sections for Kr, Xe and Rn are deeper at 30 eV than the corresponding values at 20 eV. A discussion on angular distribution has also been given by Massey and Burhop (1969).

We present in figure 12 our computed spin polarisation of elastic scattering of electrons by Kr at 20 and 30 eV. There is excellent agreement with the full relativistic work of Walker (1981). The spin–orbit splitting of the phaseshift with $l>0$ is small since the direct relativistic effect has only a small contribution. Thus the spin polarisation is small too; the peaks and dips occur near scattering angles where there are minima in the differential cross section (Kessler 1969). A formal analysis of the zeros of the spin polarisation has been given by De-Shalit (1966) and Bühring (1968).

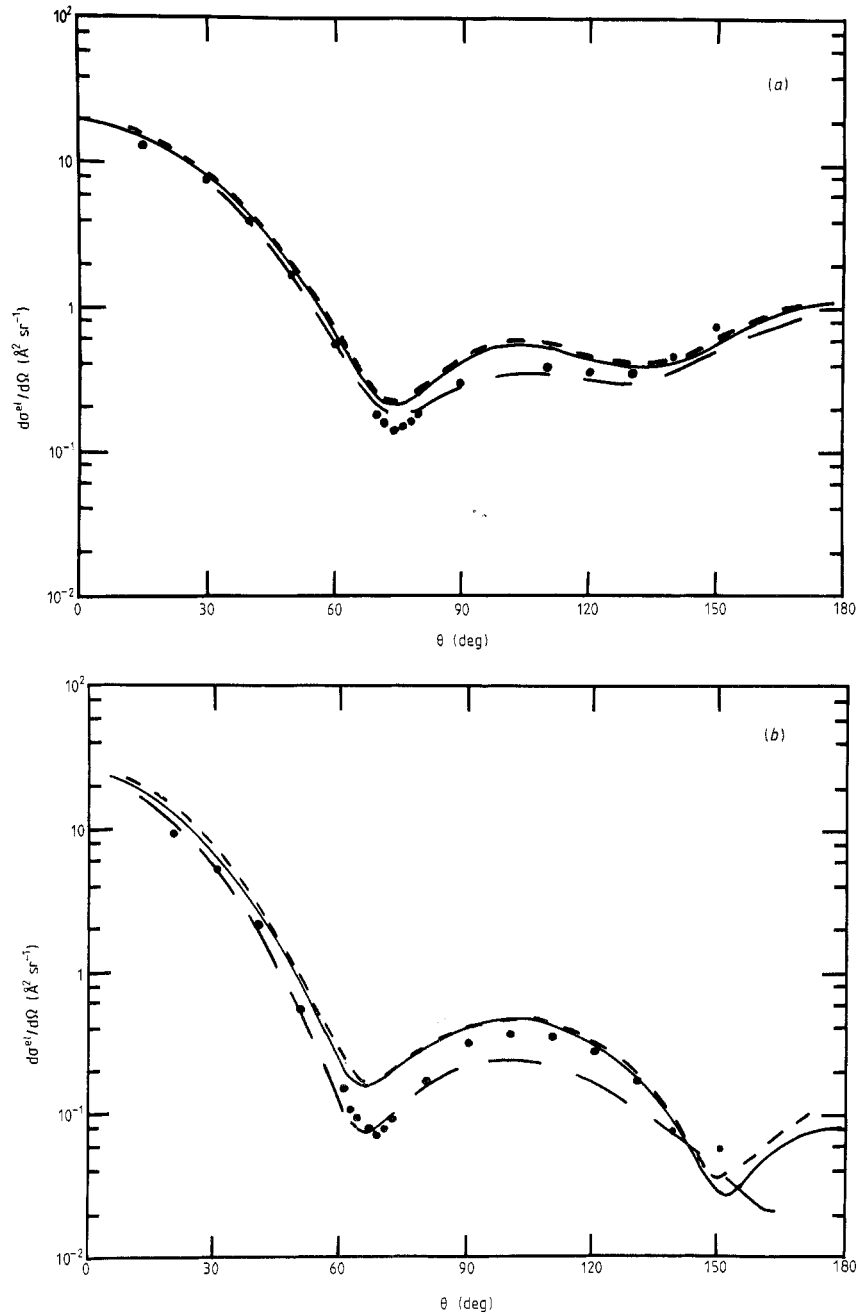

Figure 9. Elastic differential cross sections for krypton at (*a*) 20 and (*b*) 30 eV. Theory: ——, present work; – –, Walker (1981); — —, McCarthy *et al* (1977). Experiment: ●, Williams and Crowe (1975).

Figure 13 compares our results on the spin polarisation for Xe with the measurements of Klewer *et al* (1979) at energies of 25 and 30 eV, the full relativistic work of Walker (1981) at 30 eV and the non-exchange calculation of Fink and Yates (1970) at

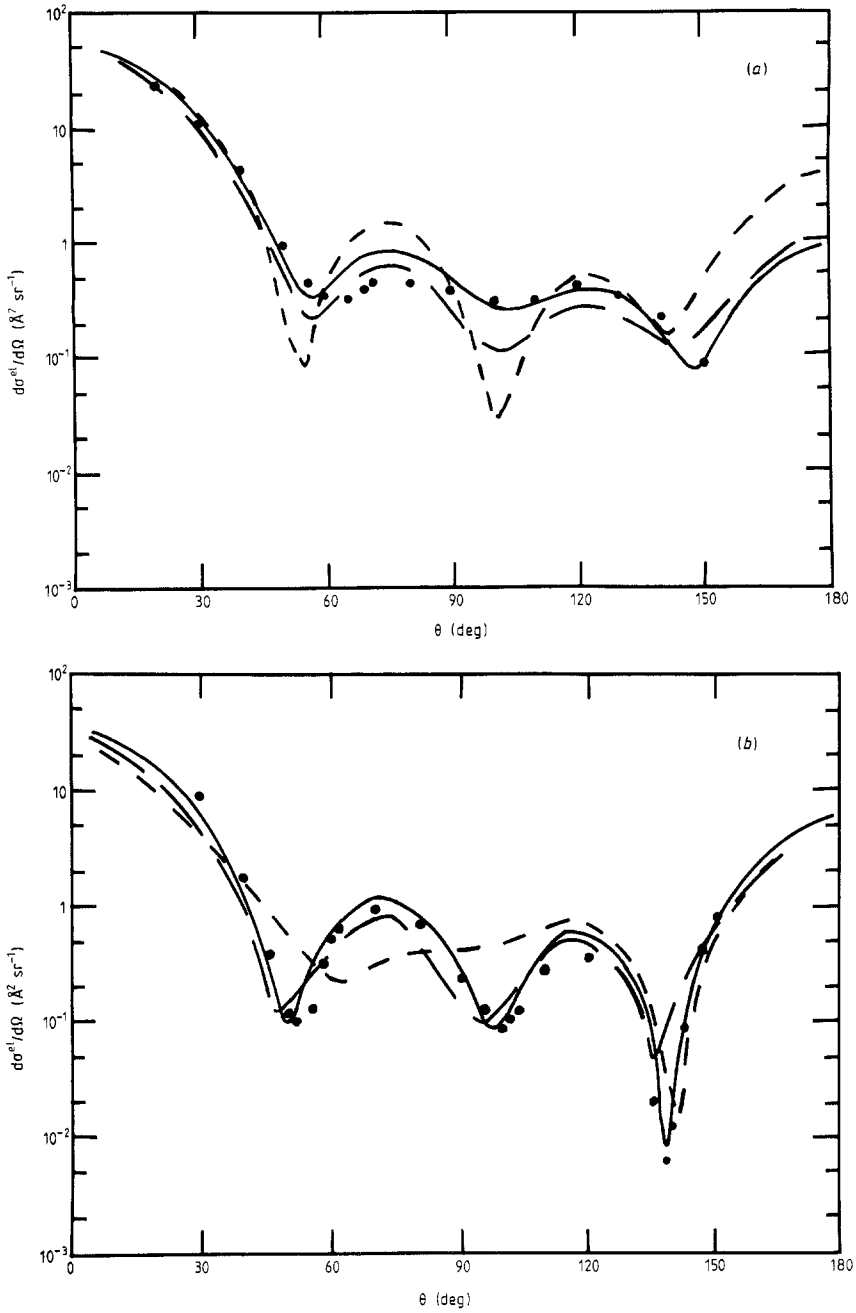

Figure 10. Elastic differential cross sections for xenon at (*a*) 20 and (*b*) 30 eV. Theory: ——, present work; – –, Walker (1981); — —, McCarthy *et al* (1977). Experiment: ●, Williams and Crowe (1975).

25 eV. Agreement between the present work and the calculation of Walker is unsatisfactory because of the large f-wave phaseshift used in his calculation. There is poor agreement between theory and experiment. In each part of the figure the error bars of

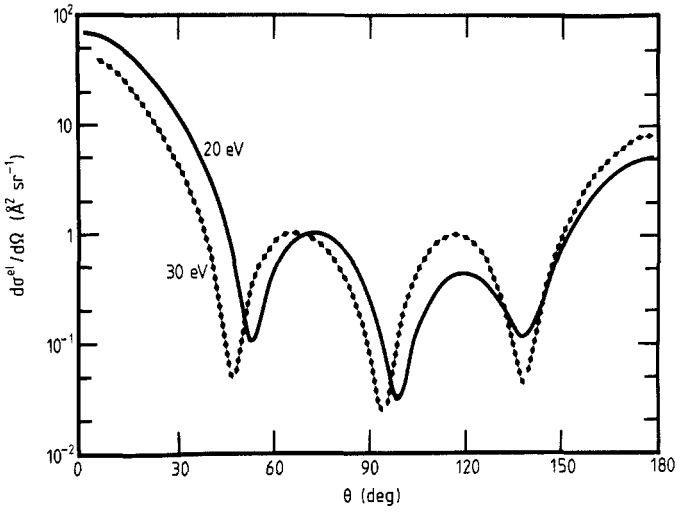

Figure 11. Elastic differential cross sections for radon at 20 and 30 eV.

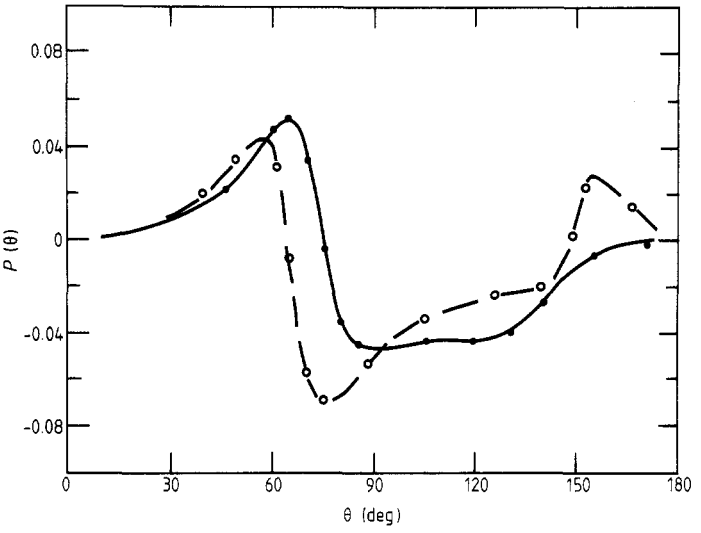

Figure 12. Spin polarisation for krypton at 20 and 30 eV. 20 eV: ——, present work; ●, Walker (1981). 30 eV: — —, present work; ○, Walker (1981).

the experimental data represent the two standard deviations (95% confidence limits) due to the statistical uncertainty in the count rates. In the experiment of Klewer *et al* the angular resolution of the spectra was estimated to be ±7° and the overall resolution was found to be about 1 eV. In view of the correlation between spin polarisation and differential cross section, and the good agreement between the present work and the experiment of Williams and Crowe (1975) on elastic differential cross sections for xenon at 30 eV, the discrepancy between calculations and measurements on the shape of the spin polarisation curve at the same energy is puzzling.

Finally, we present in figure 14 our calculated spin polarisation for Rn at energies of 20 and 30 eV. It is seen from the results shown in figures 12–14 that the magnitude of

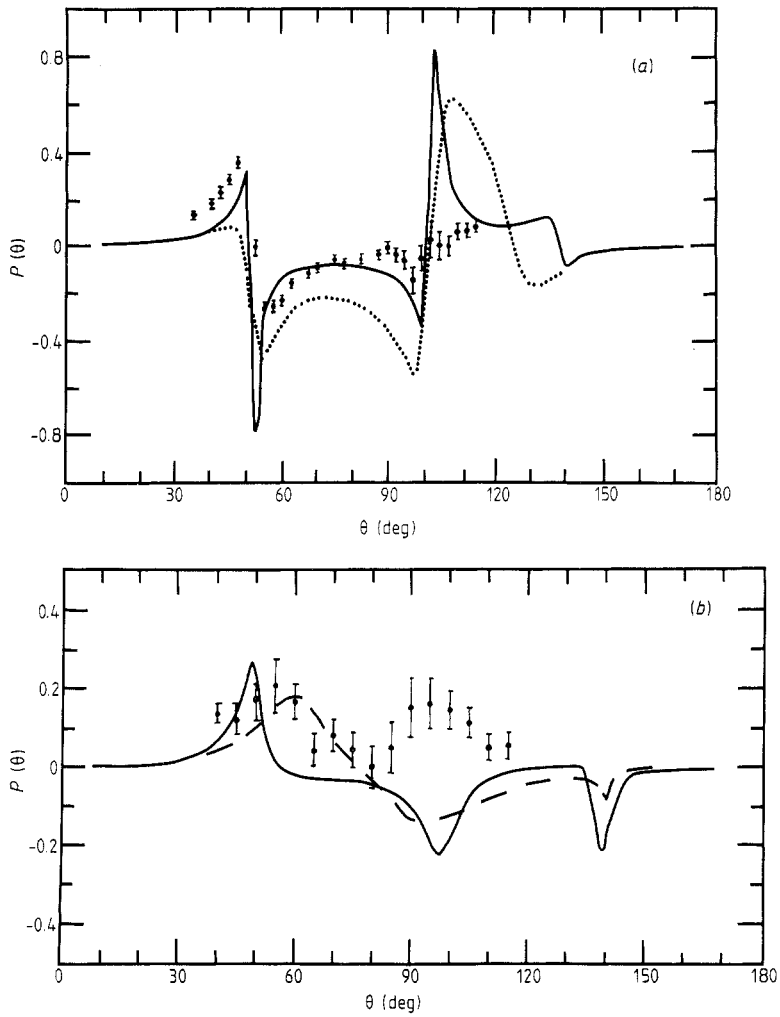

Figure 13. Spin polarisation for xenon at (*a*) 25 and (*b*) 30 eV. Experiment: ●, Klewer *et al* (1979). Theory: ——, present work; — —, Walker (1981) at 30 eV; · · · · ·, Fink and Yates (1970) at 25 eV.

the spin polarisation increases with the size of the target. This is a consequence of the contribution of the direct relativistic effect which increases with the nuclear charge of the atom.

4. Conclusions

The elastic scattering of low-energy electrons by heavy inert-gas atoms has been investigated using a semi-relativistic method which takes into account direct and indirect relativistic effects. It has been shown that the contribution from the direct effect increases with the nuclear charge of the target. There is good agreement between the present work and the full relativistic calculation of Walker, except at energies above

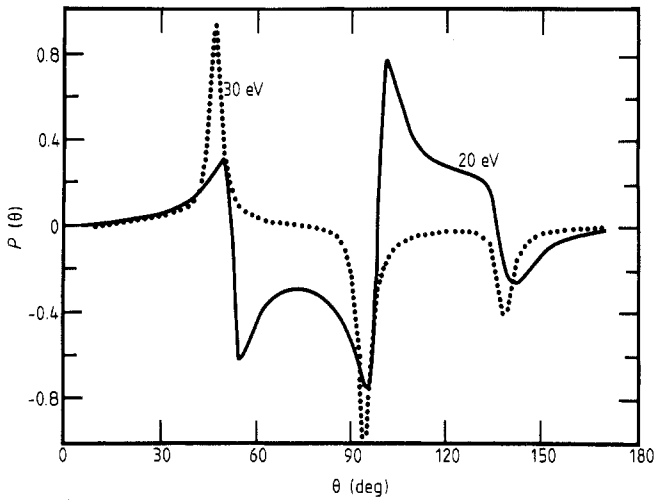

Figure 14. Spin polarisation for radon at 20 and 30 eV.

15 eV for xenon. However, the semi-relativistic method is easier to use and yields more information on the contribution of the direct relativistic effect. The present work has shown that the calculated d- and f-partial-wave phaseshifts are very sensitive to the polarisation potential used. The semi-relativistic method predicts results which are in general agreement with measurements on total, momentum-transfer and elastic differential cross sections for krypton and xenon. The poor agreement between theory and experiment on spin polarisation for xenon at energies of 25 and 30 eV indicates the need for further investigation. Finally, the calculation indicates that, in analogy with krypton and xenon, radon exhibits the Ramsauer–Townsend effect also.

Acknowledgments

The author wishes to thank Professor J F Williams and Dr D W Walker for useful discussions, and Dr R W Crompton for a critical reading of the manuscript.

References

Bransden B H and McDowell M R C 1978 *Phys. Rev.* **46** 249–394
Bühring W 1968 *Z. Phys.* **208** 286–98
Dababneh M S, Kauppila W E, Downing J P, Laperriere F, Pol V, Smart J H and Stein T S 1980 *Phys. Rev.* **22** 1872–7
De-Shalit A 1966 *Preludes in Theoretical Physics* ed A De-Shalit, H Feshbach and L van Hove (Amsterdam: North-Holland) pp 35–43
Desclaux J P 1975 *Comput. Phys. Commun.* **9** 31–45
Fink M and Yates A 1970 *Electronic Research Center Technical Report No 88* (Austin: University of Texas)
Frost L S and Phelps A V 1964 *Phys. Rev.* **136** A 1538–45
Furness J B and McCarthy I E 1973 *J. Phys. B: At. Mol. Phys.* **6** 2280–91
de Heer F J, Jansen R H J and van der Kaay W 1979 *J. Phys. B: At. Mol. Phys.* **12** 979–1002
Heindorff T, Höfft J and Dabkiewicz P 1976 *J. Phys. B: At. Mol. Phys.* **9** 89–99
Kessler J 1969 *Rev. Mod. Phys.* **41** 3–25

Kieffer L J 1971 *At. Data* **2** 293–392
Klewer M, Beerlage M J M and van der Wiel M J 1979 *J. Phys. B: At. Mol. Phys.* **12** 3935–46
McCarthy I E, Noble C J, Phillips B A and Turnbull A D 1977 *Phys. Rev.* A **15** 2173–85
McEachran R P, Stauffer A D and Greita S 1979 *J. Phys. B: At. Mol. Phys.* **12** 3119–23
Massey H S W and Burhop E H S 1969 *Electronic and Ionic Impact Phenomena* (London: Oxford University Press) vol 1, p 411
Massey H S W, Lawson J and Thompson D G 1966 *Quantum Theory of Atoms, Molecules and the Solid State* ed P Lowdin (New York: Academic) pp 203–15
Mehr J 1967 *Z. Phys.* **198** 345–50
Miller T M and Bederson B 1977 *Advances in Atomic and Molecular Physics* vol 13 (New York: Academic) pp 1–55
Mott N F 1929 *Proc. R. Soc.* A **124** 425–42
Ramsauer C 1923 *Ann. Phys., Lpz.* **72** 345–52
Ramsauer C and Kollath R 1929 *Ann. Phys., Lpz.* **3** 536–64
Sinfailam A L and Thompson D G 1971 *J. Phys. B: At. Mol. Phys.* **4** 461–7
Sin Fai Lam L T 1980 *Aust. J. Phys.* **33** 261–81
—— 1981 *J. Phys. B: At. Mol. Phys.* **14** 3543–9
—— 1982 *J. Phys. B: At. Mol. Phys.* **15** 143–53
Sin Fai Lam L T and Baylis W E 1981 *J. Phys. B: At. Mol. Phys.* **14** 559–71
Srivastava S K, Tanaka H, Chutjian A and Trajmar S 1981 *Phys. Rev.* A **23** 2156–66
Thompson D G 1971 *J. Phys. B: At. Mol. Phys.* **4** 468–82
Townsend J S and Bailey V A 1922 *Phil. Mag.* **43** 593–600
Wagenaar R W 1978 *FOM-Report* No 43948
Walker D W 1981 private communication
Williams J F and Crowe A 1975 *J. Phys. B: At. Mol. Phys.* **8** 2233–48
Yau A W, McEachran R P and Stauffer A D 1980 *J. Phys. B: At. Mol. Phys.* **13** 377–84